

World Journal of *Gastrointestinal Oncology*

World J Gastrointest Oncol 2024 October 15; 16(10): 4037-4299



EDITORIAL

- 4037 Improving clinical outcomes of patients with hepatocellular carcinoma: Role of antiviral therapy, conversion therapy, and palliative therapy
Shelat VG
- 4042 Unresectable hepatocellular carcinoma: Transarterial chemoembolization combined with lenvatinib in combination with programmed death-1 inhibition is a possible approach
Zhao FY, Wang DY, Qian NS
- 4045 Advances in endoscopic diagnosis and management of colorectal cancer
Li SW, Liu X, Sun SY
- 4052 Multidisciplinary approaches in the management of advanced hepatocellular carcinoma: Exploring future directions
Liu XJ, Lin YX, Chen LX, Yang WJ, Hu B
- 4055 Clinical implications of the latest advances in gastrointestinal tumor research
Dai W, Li YQ, Zhou Y
- 4060 Targeting methyltransferase-like 5-mediated sphingomyelin metabolism: A novel therapeutic approach in gastric cancer
Zhang JJ, Yuan C, Dang SC

REVIEW

- 4064 Research progress of tumor-associated macrophages in immune checkpoint inhibitor tolerance in colorectal cancer
Fan Q, Fu ZW, Xu M, Lv F, Shi JS, Zeng QQ, Xiong DH

MINIREVIEWS

- 4080 Update understanding on diagnosis and histopathological examination of atrophic gastritis: A review
Ma XZ, Zhou N, Luo X, Guo SQ, Mai P

ORIGINAL ARTICLE**Retrospective Cohort Study**

- 4092 Establishing prognostic models for intrahepatic cholangiocarcinoma based on immune cells
Wang ZR, Zhang CZ, Ding Z, Li YZ, Yin JH, Li N

Retrospective Study

- 4104** Constructing a nomogram to predict overall survival of colon cancer based on computed tomography characteristics and clinicopathological factors
Hu ZX, Li Y, Yang X, Li YX, He YY, Niu XH, Nie TT, Guo XF, Yuan ZL
- 4115** Computed tomography-based radiomic model for the prediction of neoadjuvant immunochemotherapy response in patients with advanced gastric cancer
Zhang J, Wang Q, Guo TH, Gao W, Yu YM, Wang RF, Yu HL, Chen JJ, Sun LL, Zhang BY, Wang HJ
- 4129** Characteristics and risk factor analyses of high-grade intraepithelial neoplasia in older patients with colorectal polyps
Zhang X, Wang Y, Zhu T, Ge J, Yuan JH
- 4138** Clinicopathological analysis of small intestinal metastasis from extra-abdominal/extra-pelvic malignancy
Zhang Z, Liu J, Yu PF, Yang HR, Li JY, Dong ZW, Shi W, Gu GL
- 4146** Uninvolved liver dose prediction in stereotactic body radiation therapy for liver cancer based on the neural network method
Zhang HW, Wang YH, Hu B, Pang HW

Observational Study

- 4157** Small particle drug-eluting beads-transarterial chemoembolization combined with targeted therapy in the clinical treatment of unresectable liver cancer
Qi JS, Zhao P, Zhao XB, Zhao YL, Guo YC
- 4166** Nationwide questionnaire survey on pediatric pancreatic tumors in Japan
Makita S, Uchida H, Kano M, Kawakubo N, Miyake H, Yoneda A, Tajiri T, Fukumoto K

Clinical and Translational Research

- 4177** Burden landscape of hepatobiliary and pancreatic cancers in Chinese young adults: 30 years' overview and forecasted trends
Chen DS, Chen ZP, Zhu DZ, Guan LX, Zhu Q, Lou YC, He ZP, Chen HN, Sun HC

Basic Study

- 4194** Long noncoding RNA steroid receptor RNA activator 1 inhibits proliferation and glycolysis of esophageal squamous cell carcinoma
He M, Qi Y, Zheng ZM, Sha M, Zhao X, Chen YR, Chen ZH, Qian RY, Yao J, Yang ZD
- 4209** Jianpi-Huatan-Huoxue-Anshen formula ameliorates gastrointestinal inflammation and microecological imbalance in chemotherapy-treated mice transplanted with H22 hepatocellular carcinoma
Wang YN, Zhai XY, Wang Z, Gao CL, Mi SC, Tang WL, Fu XM, Li HB, Yue LF, Li PF, Xi SY
- 4232** Intratumoural microorganism can affect the progression of hepatocellular carcinoma
Liu BQ, Bai Y, Chen DP, Zhang YM, Wang TZ, Chen JR, Liu XY, Zheng B, Cui ZL

- 4244** Clinical significance of upregulated Rho GTPase activating protein 12 causing resistance to tyrosine kinase inhibitors in hepatocellular carcinoma
Wang XW, Tang YX, Li FX, Wang JL, Yao GP, Zeng DT, Tang YL, Chi BT, Su QY, Huang LQ, Qin DY, Chen G, Feng ZB, He RQ

CASE REPORT

- 4264** Rare and lacking typical clinical symptoms of liver tumors: Four case reports
Zhao Y, Bie YK, Zhang GY, Feng YB, Wang F
- 4274** Conversion therapy in advanced perihilar cholangiocarcinoma based on patient-derived organoids: A case report
He YG, Zhang LY, Li J, Wang Z, Zhao CY, Zheng L, Huang XB
- 4281** Transformed gastric mucosa-associated lymphoid tissue lymphoma originating in the colon and developing metachronously after *Helicobacter pylori* eradication: A case report
Saito M, Tanei ZI, Tsuda M, Suzuki T, Yokoyama E, Kanaya M, Izumiyama K, Mori A, Morioka M, Kondo T

LETTER TO THE EDITOR

- 4289** Conversion therapy for unresectable hepatocellular carcinoma: Advances and challenges
He YF

CORRECTION

- 4298** Correction to “Research progress of ferroptosis regulating lipid peroxidation and metabolism in occurrence of primary liver cancer”
Shu YJ, Lao B, Qiu YY

ABOUT COVER

Editorial Board of *World Journal of Gastrointestinal Oncology*, Gaetano Piccolo, MD, PhD, Doctor, Department of Health Sciences, University of Milan, San Paolo Hospital, Via Antonio di Rudini 8, Milan 20142, Lombardy, Italy. gpiccolo1983@gmail.com

AIMS AND SCOPE

The primary aim of *World Journal of Gastrointestinal Oncology* (*WJGO*, *World J Gastrointest Oncol*) is to provide scholars and readers from various fields of gastrointestinal oncology with a platform to publish high-quality basic and clinical research articles and communicate their research findings online.

WJGO mainly publishes articles reporting research results and findings obtained in the field of gastrointestinal oncology and covering a wide range of topics including liver cell adenoma, gastric neoplasms, appendiceal neoplasms, biliary tract neoplasms, hepatocellular carcinoma, pancreatic carcinoma, cecal neoplasms, colonic neoplasms, colorectal neoplasms, duodenal neoplasms, esophageal neoplasms, gallbladder neoplasms, *etc.*

INDEXING/ABSTRACTING

The *WJGO* is now abstracted and indexed in PubMed, PubMed Central, Science Citation Index Expanded (SCIE, also known as SciSearch®), Journal Citation Reports/Science Edition, Scopus, Reference Citation Analysis, China Science and Technology Journal Database, and Superstar Journals Database. The 2024 edition of Journal Citation Reports® cites the 2023 journal impact factor (JIF) for *WJGO* as 2.5; JIF without journal self cites: 2.5; 5-year JIF: 2.8; JIF Rank: 71/143 in gastroenterology and hepatology; JIF Quartile: Q2; and 5-year JIF Quartile: Q2. The *WJGO*'s CiteScore for 2023 is 4.2 and Scopus CiteScore rank 2023: Gastroenterology is 80/167; Oncology is 196/404.

RESPONSIBLE EDITORS FOR THIS ISSUE

Production Editor: *Si Zhao*; Production Department Director: *Xiang Li*; Cover Editor: *Jia-Ru Fan*.

NAME OF JOURNAL

World Journal of Gastrointestinal Oncology

ISSN

ISSN 1948-5204 (online)

LAUNCH DATE

February 15, 2009

FREQUENCY

Monthly

EDITORS-IN-CHIEF

Monjur Ahmed, Florin Burada

EDITORIAL BOARD MEMBERS

<https://www.wjgnet.com/1948-5204/editorialboard.htm>

PUBLICATION DATE

October 15, 2024

COPYRIGHT

© 2024 Baishideng Publishing Group Inc

INSTRUCTIONS TO AUTHORS

<https://www.wjgnet.com/bpg/gerinfo/204>

GUIDELINES FOR ETHICS DOCUMENTS

<https://www.wjgnet.com/bpg/GerInfo/287>

GUIDELINES FOR NON-NATIVE SPEAKERS OF ENGLISH

<https://www.wjgnet.com/bpg/gerinfo/240>

PUBLICATION ETHICS

<https://www.wjgnet.com/bpg/GerInfo/288>

PUBLICATION MISCONDUCT

<https://www.wjgnet.com/bpg/gerinfo/208>

ARTICLE PROCESSING CHARGE

<https://www.wjgnet.com/bpg/gerinfo/242>

STEPS FOR SUBMITTING MANUSCRIPTS

<https://www.wjgnet.com/bpg/GerInfo/239>

ONLINE SUBMISSION

<https://www.f6publishing.com>



Retrospective Study

Computed tomography-based radiomic model for the prediction of neoadjuvant immunotherapy response in patients with advanced gastric cancer

Jun Zhang, Qi Wang, Tian-Hui Guo, Wen Gao, Yi-Miao Yu, Rui-Feng Wang, Hua-Long Yu, Jing-Jing Chen, Ling-Ling Sun, Bi-Yuan Zhang, Hai-Ji Wang

Specialty type: Gastroenterology and hepatology

Provenance and peer review:

Unsolicited article; Externally peer reviewed.

Peer-review model: Single blind

Peer-review report's classification

Scientific Quality: Grade C, Grade D

Novelty: Grade B, Grade C

Creativity or Innovation: Grade C, Grade C

Scientific Significance: Grade C, Grade C

P-Reviewer: Yang JP

Received: May 16, 2024

Revised: August 18, 2024

Accepted: August 28, 2024

Published online: October 15, 2024

Processing time: 132 Days and 18.8 Hours



Jun Zhang, Qi Wang, Tian-Hui Guo, Wen Gao, Yi-Miao Yu, Rui-Feng Wang, Bi-Yuan Zhang, Hai-Ji Wang, Department of Radiation Oncology, Affiliated Hospital of Qingdao University, Qingdao 266000, Shandong Province, China

Hua-Long Yu, Jing-Jing Chen, Department of Radiology, Affiliated Hospital of Qingdao University, Qingdao 266000, Shandong Province, China

Ling-Ling Sun, Department of Pathology, Affiliated Hospital of Qingdao University, Qingdao 266000, Shandong Province, China

Co-corresponding authors: Bi-Yuan Zhang and Hai-Ji Wang.

Corresponding author: Hai-Ji Wang, MD, PhD, Associate Chief Doctor, Associate Professor, Department of Radiation Oncology, Affiliated Hospital of Qingdao University, No. 59 Haier Road, Laoshan District, Qingdao 266000, Shandong Province, China. wanghaiji@qdu.edu.cn

Abstract

BACKGROUND

Neoadjuvant immunotherapy (nICT) has emerged as a popular treatment approach for advanced gastric cancer (AGC) in clinical practice worldwide. However, the response of AGC patients to nICT displays significant heterogeneity, and no existing radiomic model utilizes baseline computed tomography to predict treatment outcomes.

AIM

To establish a radiomic model to predict the response of AGC patients to nICT.

METHODS

Patients with AGC who received nICT ($n = 60$) were randomly assigned to a training cohort ($n = 42$) or a test cohort ($n = 18$). Various machine learning models were developed using selected radiomic features and clinical risk factors to predict the response of AGC patients to nICT. An individual radiomic nomogram was established based on the chosen radiomic signature and clinical signature. The performance of all the models was assessed through receiver operating characteristic curve analysis, decision curve analysis (DCA) and the Hosmer-

Lemeshow goodness-of-fit test.

RESULTS

The radiomic nomogram could accurately predict the response of AGC patients to nICT. In the test cohort, the area under curve was 0.893, with a 95% confidence interval of 0.803-0.991. DCA indicated that the clinical application of the radiomic nomogram yielded greater net benefit than alternative models.

CONCLUSION

A nomogram combining a radiomic signature and a clinical signature was designed to predict the efficacy of nICT in patients with AGC. This tool can assist clinicians in treatment-related decision-making.

Key Words: Gastric cancer; Radiomics; Computed tomography; Neoadjuvant immunochemotherapy; Machine learning; Immunology

©The Author(s) 2024. Published by Baishideng Publishing Group Inc. All rights reserved.

Core Tip: We developed and validated a prediction model based on a radiomic signature and a clinical signature to assess the tumor regression grade in advanced gastric cancer (AGC) patients receiving neoadjuvant immunochemotherapy (nICT). The radiomic nomogram showed strong performance in predicting the tumor regression grade in both the training and internal test cohorts. This study represents the first application of radiomics for predicting the nICT response in AGC patients.

Citation: Zhang J, Wang Q, Guo TH, Gao W, Yu YM, Wang RF, Yu HL, Chen JJ, Sun LL, Zhang BY, Wang HJ. Computed tomography-based radiomic model for the prediction of neoadjuvant immunochemotherapy response in patients with advanced gastric cancer. *World J Gastrointest Oncol* 2024; 16(10): 4115-4128

URL: <https://www.wjgnet.com/1948-5204/full/v16/i10/4115.htm>

DOI: <https://dx.doi.org/10.4251/wjgo.v16.i10.4115>

INTRODUCTION

Gastric cancer (GC) had the fifth highest global incidence and mortality rate in 2022[1]. Significant advancements have been achieved in the current diagnostic and therapeutic tools for GC, and of these, surgery remains the primary curative treatment option[2]. Several clinical trials have focused on improving the prognosis of advanced GC (AGC) patients and have verified that neoadjuvant therapy for patients with locally AGC can decrease tumor size, increase the likelihood of achieving R0 resection, and decrease the chances of postoperative recurrence. These findings suggest that neoadjuvant therapy combined with surgery can lead to improved outcomes for patients compared with surgery alone[3,4]. Furthermore, advancements in medicine have led to the increasing approval of immunotherapy in clinical settings, which has significantly altered the landscape of tumor treatment[5]. Immunotherapy has also had exciting success in the treatment of GC, and several studies have demonstrated that the combination of a programmed death (PD)-1 inhibitor with chemotherapy significantly improves progression-free survival (PFS) and overall survival (OS) in patients with a programmed cell death 1 ligand 1 (PD-L1) combined positive score (CPS) > 5[6,7]. Two KEYNOTE trials have demonstrated the effectiveness of immune checkpoint inhibitors (ICIs) in patients diagnosed with metastatic GC[8,9]. Immunotherapy is now widely acknowledged as the preferred first-line treatment for AGC worldwide. However, the potential benefits of immunotherapy in the initial stages of GC treatment, specifically in the neoadjuvant phase, are currently under scrutiny. Clinical trials, such as NCT04354662, NCT04119622, and NCT04694183, have explored the combination of immunotherapy with chemotherapy as a neoadjuvant therapy for GC. A meta-analysis of five articles involving 206 patients indicated that neoadjuvant immunochemotherapy (nICT) shows promise as a recommended treatment strategy for AGC patients. Compared with neoadjuvant chemotherapy, nICT results in higher rates of pathological complete response (pCR), major pathologic response (MPR), and R0 resection[10].

Computed tomography (CT) has become a standard tool in clinical practice, but traditional measurements and criteria such as RECIST and iRECIST are inadequate for predicting the response to ICIs and hinder the progress of precision medicine[11]. Radiomics provides a valuable method for extracting detailed data from CT images to capture textural features that may not have been clinically observable in the past[12]. The process of radiomics involves several key steps, and the choice of methodology at each stage plays a crucial role in determining the quality of the final model[13]. Significant advancements have been made in radiomics research within the realms of clinical cancer diagnosis, treatment, and assessment. For example, radiomic features have been utilized to predict therapeutic response in patients with lung cancer[14], predict the recurrence of hepatocellular carcinoma[15], and predict survival in patients with esophageal cancer receiving definitive chemoradiotherapy[16].

Radiomics has been extensively utilized in the field of GC to predict the response to various treatments, including neoadjuvant chemotherapy, ICI therapy, and palliative chemotherapy, with area under the curve (AUC) values ranging from 0.74 to 0.82[17-20]. However, the prognostic significance of radiomic features in GC patients receiving nICT remains

to be investigated. Therefore, this study sought to develop a radiomic model specifically to predict the response of AGC patients to nICT.

MATERIALS AND METHODS

Patient screening and study design

This study was approved by the Institutional Review Committee of the Affiliated Hospital of Qingdao University. Written informed consent was waived because of the retrospective nature of the study. Data from patients with AGC who received nICT between 2020 and 2023 at the Affiliated Hospital of Qingdao University, China, were collected. The inclusion criteria were as follows: (1) Histologically confirmed gastric adenocarcinoma; (2) Treatment with at least 2 cycles of nICT; (3) Available data on baseline enhanced abdominal CT scans performed < 30 days before nICT treatment; (4) Radical surgery performed within 1 month after the end of nICT treatment; and (5) Complete postoperative pathological data. The exclusion criteria were as follows: (1) Lesions that could not be clearly displayed on CT images or metastatic lesions that could not be measured or evaluated; (2) The presence of other primary tumors; (3) No surgery after neoadjuvant therapy and incomplete pathological data; and (4) Presence of distant metastases. Of the 96 patients initially included, 15 lacked baseline CT images, 9 received fewer than 2 cycles of nICT, and 12 of the remaining 72 patients ultimately failed to undergo standard radical surgery. A flowchart of patient enrollment is shown in [Figure 1](#). Finally, 60 patients were included. The following clinicopathological data were collected: Age, sex, treatment regimen, number of nICT cycles, degree of differentiation, carcinoembryonic antigen (CEA), carbohydrate antigen199 (CA199), clinical T (cT) stage, clinical N (cN) stage and PD-L1 status. Patients with a PD-L1 CPS \geq 5 were classified as PD-L1-positive.

In all, 60 patients were assigned to two datasets (42 patients in the training dataset and 18 patients in the validation dataset) *via* computer-generated random numbers at a ratio of 7:3. All patients received nICT treatment. All patients received chemotherapy regimens recommended by the National Comprehensive Cancer Network or the American Society of Clinical Oncology for neoadjuvant chemotherapy in AGC. For immunotherapy regimens, 15 patients received serplulimab, 22 patients received camrelizumab, 11 patients received sintilimab, 9 patients received nivolumab, 2 patients received tislelizumab, and 1 patient received toripalimab. All patients underwent radical surgery within one month after the last cycle of nICT.

CT examination

Contrast-enhanced abdominal CT scans were performed with a six-hour fasting protocol in all patients. All CT examinations were performed on a 64-detector row scanner using the GE MEDICAL SYSTEMS Optima CT620/670 or the Siemens SOMATOM definition flash. The CT scan parameters included 120 kVp as the tube energy and 5 mm as the slice thickness. Patients were scanned in the supine position, and the area from the diaphragmatic dome to 2 cm below the lower margin of the symphysis pubis was covered. A total of 1.5 mL/kg of nonionic contrast material (iohexol 300 mg/mL, Omnipaque, GE Healthcare) was administered at a rate of 3.5 mL/s through the antecubital vein *via* a high-pressure injector. The arterial and venous phases were scanned at 40 s and 70 s, respectively, after contrast media injection.

Evaluation of treatment efficacy

Patient treatment response was evaluated according to the tumor regression grade (TRG), as described in the 8th edition of the American joint committee on cancer. TRG grade 0 was defined as no remaining cancer cells (complete regression), and TRG grade 1 was defined as the observation of only single cancer cells or clusters of cancer cells (almost complete regression). According to the postoperative pathology report, patients with TRG grades 0-1 were classified as responders ($n = 15$), while patients with TRG grades 2-3 were classified as nonresponders ($n = 45$)[\[21\]](#). Histopathological findings were assessed by a pathologist with at least 10 years of experience in diagnosing gastric disease.

Radiomic prediction model

Image analysis and segmentation: The tumor lesion was more clearly visible and distinguishable from the normal peripheral tissue in the portal venous phase, which has been commonly utilized for tumor segmentation in previous studies[\[22,23\]](#). Two experienced gastrointestinal radiologists, Yu HL with 20 years of experience and Chen JJ with 10 years of experience, independently analyzed the baseline CT scans in the venous phase. Both radiologists were blinded to the clinical and histopathological information but were aware of the anatomical location of the GC. Intratumoral regions of interest (ROIs) were manually contoured on venous phase images of the gastric lesions in the axial plane *via* ITK-SNAP software (v.3.8.0, <http://www.itksnap.org>). The primary tumor region was manually delineated and defined as the ROI. Radiologists 1 (Yu YM, with 20 years of experience) and 2 (Chen JJ, with 10 years of experience) delineated the ROIs for all 60 AGC patients, and any differences were resolved by consensus. To ensure reproducibility, we randomly selected 15 patients and had the two radiologists mentioned above redraw their ROIs one month later for feature extraction. The results were analyzed to detect any intra observer differences that could impact radiomic feature reproducibility.

Radiomic feature extraction and selection: Radiomic features were extracted *via* the PyRadiomics package (version 3.0.1). The reproducibility and robustness of the extracted radiomic features were evaluated using intraclass and interclass correlation coefficients (ICCs). Only radiomic features with an ICC value of 0.8 or higher were considered stable and retained for further analysis. The CT images and ROIs were resampled and standardized *via* RIAS software (version 0.2.1)[\[24\]](#).

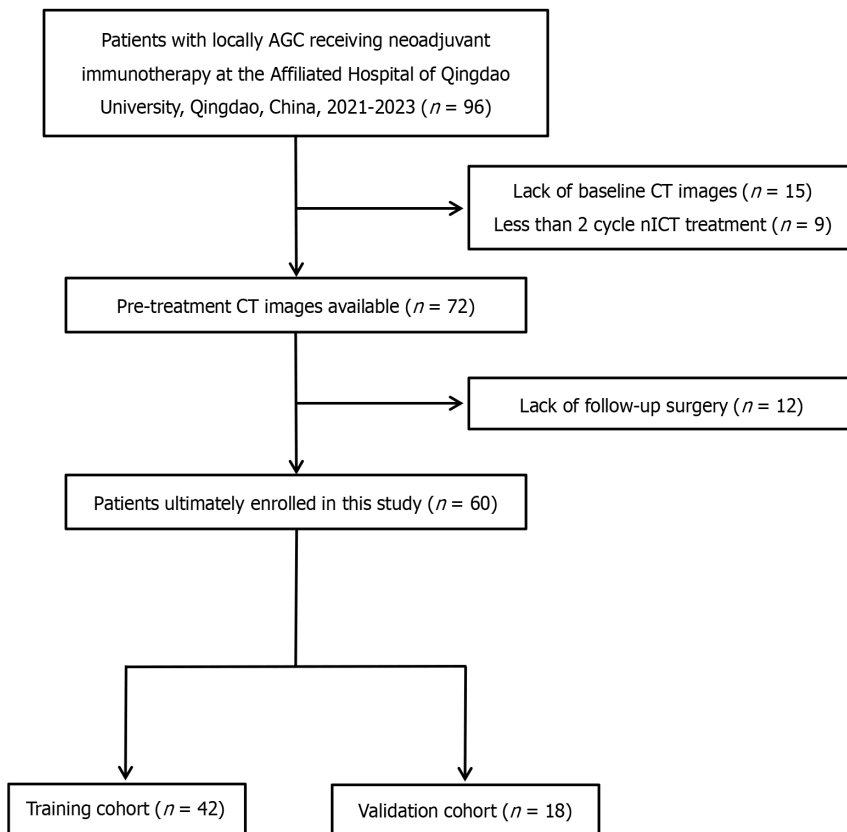


Figure 1 A flow chart of patient enrollment. AGC: Advanced gastric cancer; CT: Computed tomography; nICT: Neoadjuvant immunochemotherapy.

In all, 1834 radiomic features were selected and categorized into first-order, shape, texture, and wavelet features. Features with a significance level of $P < 0.05$ were initially identified by an independent samples t test. Subsequently, features that displayed a high level of correlation ($P > 0.9$) were removed. To standardize the radiomic feature data in both the training and test cohorts, Z score normalization was applied. In the training cohort, the least absolute shrinkage and selection operator (LASSO) regression technique was employed for feature selection and the construction of a radiomic signature (rad-signature). A 5-fold cross-validation approach was used to determine the regularization parameter λ .

Radiomic signature establishment: Multiple machine learning radiomic models, including logistic regression (LR), K-nearest neighbor (KNN) classification, random forest (RF), extra trees, eXtreme gradient boosting (XGBoost), multilayer perceptron (MLP) and support vector machine (SVM) models, were built according to the selected radiomic features. Finally, the radiomic signature and a formula were developed; the signature score was calculated as the sum of the values of the selected features multiplied by their respective coefficients. The prognostic value of the radiomic signature in patients with AGC treated with nICT was assessed according to the receiver operating characteristic (ROC) curve. Decision curves were employed to evaluate the model predictions and to determine the net benefit of an intervention based on the model outcomes.

Clinical signature establishment

Baseline clinical data, including age, sex, treatment regimen, number of nICT cycles, degree of differentiation, PD-L1 status, CEA level, CA199 level, cT stage and cN stage, were extracted from the hospital's medical records. According to the eighth tumor node metastasis staging criteria, T indicates the extent of the primary tumor, whereas N represents the existence and extent of regional lymph node metastasis. To investigate factors that contribute to the nICT response, we compared clinical risk factors (age, sex, primary tumor location) and molecular biomarkers (PD-L1, CEA, CA199) between responders ($n = 15$) and nonresponders ($n = 45$) (Table 1). Our findings suggest that pretreatment cN stage and pretreatment cT stage are significant clinical risk factors ($P < 0.05$) that influence the nICT response (Table 1). However, previous studies have shown that PD-L1 expression, cT stage, cN stage, tumor differentiation, and tumor location may be correlated with the immunotherapy response in patients with GC[25-27]. Multiple machine learning clinical models, including the LR, KNN classification, RF, extra trees, XGBoost, MLP and SVM models, were subsequently constructed on the basis of the clinical features mentioned above. Finally, the clinical signature and a formula were developed. These models were also evaluated *via* ROC curves and decision curves.

Nomogram construction and validation

A nomogram that combines the rad-signature and the clinical signature was constructed. The discrimination performance

Table 1 Comparison of clinical characteristics between responders and non-responders, n (%)

| Characteristics | Responders (n = 15) | Non-responders (n = 45) | P value |
|----------------------------------|---------------------|-------------------------|---------|
| Age (years), average (mean ± SD) | 57.53 (12.710) | 58.64 (11.682) | 0.756 |
| Sex | | | 0.856 |
| Male | 12 (80.0) | 35 (77.8) | |
| Female | 3 (20.0) | 10 (22.2) | |
| Treatment cycles | | | 0.579 |
| 2 | 2 (13.3) | 8 (17.8) | |
| 3 | 9 (60.0) | 20 (44.4) | |
| 4 + | 4 (26.7) | 17 (37.8) | |
| Differentiation | | | 0.526 |
| High | 1 (6.7) | 1 (2.2) | |
| Moderate | 5 (33.3) | 11 (24.4) | |
| Poor | 9 (60.0) | 33 (73.3) | |
| Primary tumor location | | | 0.977 |
| Cardia | 3 (20.0) | 8 (17.8) | |
| Body | 6 (40.0) | 16 (35.6) | |
| Antrum | 4 (26.7) | 14 (31.1) | |
| Horn | 2 (13.3) | 7 (15.6) | |
| PD-L1(22C3) CPS | | | 0.237 |
| ≥ 5 | 10 (66.7) | 26 (57.8) | |
| < 5 | 5 (33.3) | 19 (42.2) | |
| CEA, median (IQR) | 2.84 (0.93-17.84) | 4.15 (1.75-9.52) | 0.706 |
| CA199, median (IQR) | 9.08 (3.85-28.89) | 16.23 (8.37-37.61) | 0.264 |
| T stage | | | 0.004 |
| 1 | 4 (26.7) | 0 (0) | |
| 2 | 1 (6.7) | 4 (8.9) | |
| 3 | 3 (20.0) | 18 (40.0) | |
| 4 | 7 (46.7) | 23 (51.1) | |
| N stage | | | 0.044 |
| 0 | 0 (0) | 1 (2.2) | |
| 1 | 11 (73.3) | 18 (40.0) | |
| 2 | 4 (26.7) | 18 (40.0) | |
| 3 | 0 (0) | 8 (17.8) | |

The P value indicates a statistically significant difference between the responder and non-responder groups ($P < 0.05$). Responders: Patients with tumor regression grade 0-1 grade; Non-responders: Patients with tumor regression grade 2-3 grade; IQR: Interquartile range; CEA: Carcinoembryonic antigen; CA199: Carbohydrate antigen 19-9; PD-L1: Programmed death-ligand 1; CPS: Combined positive score.

of the nomogram was assessed *via* ROC curves in both the training and test cohorts. Decision curves were employed to evaluate the nomogram predictions and to determine the net benefit of an intervention based on the nomogram outcomes. The Hosmer-Lemeshow goodness-of-fit test was used to evaluate the calibration ability of the nomogram.

Statistical analysis

All the statistical tests were performed *via* Python 3.7 and R software (version 4.3.0). Independent *t* tests were used for continuous variables, whereas χ^2 tests were used for categorical variables. The LASSO regression model was assessed using the “Glmnet” package, followed by the generation of ROC curves and decision curves using the “Proc” and “Dca”.

R software packages, respectively. The predictive performance of the model was evaluated according to the AUC, which serves as an indicator of predictive accuracy. Decision curves were employed to evaluate the model predictions and to determine the net benefit of an intervention based on the model outcomes. The Hosmer-Lemeshow goodness-of-fit test was used to evaluate the calibration ability of the nomogram. A significance level of $P < 0.05$ was considered statistically significant for all analyses, and two-sided tests were conducted. The Check list for the evaluation of radiomics research [28] is provided in [Supplementary Figure 1](#).

RESULTS

Patient characteristics

The characteristics of the GC patients are shown in [Table 2](#); the patients were randomly divided into a training cohort ($n = 42$, mean age: 58.26 ± 11.847 years) comprising 33 males and 9 females and a test cohort ($n = 18$, mean age 58.61 ± 12.186 years) comprising 14 males and 4 females. No statistically significant differences were observed in clinical features such as age, sex, tumor location, CEA level, CA-199 level, treatment period, cT stage or cN stage between the training and test cohorts ($P > 0.05$).

Radiomic signature

The workflow for selecting radiomic features is depicted in [Figure 2](#). The primary tumor region was manually delineated and defined as the ROI. Following the extraction of essential radiomic features and the exclusion of those with ICCs less than 0.8, 1834 radiomic features were utilized for subsequent analyses. The independent samples t test identified 199 features with $P < 0.05$, 76 of which had a $P < 0.9$. The P values were subjected to adjustment for multiple comparisons with the false discovery rate algorithm. LASSO regression was performed for these 76 features, and the 19 most meaningful features were identified ([Figure 3](#)). Multiple machine learning models, including the LR, KNN, RF, extra trees, XGBoost, MLP and SVM models, were constructed on the basis of the selected radiomic features to predict the response of AGC patients to nICT. In the training set, the AUC values of the LR, SVM, KNN, RF, extra trees, XGBoost and MLP methods were 1.000, 1.000, 0.897, 1.000, 1.000, 1.000 and 0.952, respectively. In the test set, the AUC values of the LR, SVM, KNN, RF, extra trees, XGBoost and MLP methods were 0.786, 0.750, 0.821, 0.679, 0.616, 0.75 and 0.768, respectively. Although the LR, KNN and MLP models performed well in terms of AUC values, they did not perform as well as the XGBoost model in terms of negative predictive value and positive predictive value. When the results of accuracy, AUC, sensitivity and specificity were combined, we concluded that the XGBoost model had the best performance. The XGBoost model achieved an AUC of 1.000 [95% confidence interval (CI): 1.000-1.000] in the training set and 0.750 (95%CI: 0.435-1.000) in the test set. The ROC curves for the XGBoost model are illustrated in [Figure 4A](#) and [B](#), with additional comparison results provided in [Table 3](#). The XGBoost model was selected for computing the rad-signature score for each patient, with the rad-signature formulas detailed in [Supplementary Figure 2](#).

Clinical signature

To explore the clinical risk factors that affect treatment response, we compared the clinical characteristics of responders and non-responders. Our findings suggest that pretreatment cN stage and pretreatment cT stage are significant clinical risk factors ($P < 0.05$) that influence the nICT response ([Table 1](#)). However, previous studies have shown that PD-L1 expression, cT stage, cN stage, tumor differentiation, and tumor location may be correlated with the immunotherapy response in patients with GC[25-27]. Therefore, we developed clinical models based on major clinical risk factors, including PD-L1 expression, cT stage, cN stage, tumor differentiation, and tumor location, *via* the machine learning methods mentioned above. In the training set, the AUC values of the LR, SVM, KNN, RF, extra trees, XGBoost and MLP methods were 0.837, 0.151, 0.787, 0.993, 0.999, 0.937 and 0.820, respectively. In the test set, the AUC values of the LR, SVM, KNN, RF, extra trees, XGBoost and MLP methods were 0.482, 0.571, 0.607, 0.688, 0.589, 0.696 and 0.429, respectively. Additional comparison results can be found in [Table 4](#). When the results of accuracy, AUC, sensitivity and specificity were combined, we concluded that the XGBoost model had the best performance. The XGBoost model was subsequently selected for determining the clinical signature score for each individual patient ([Figure 4C](#) and [D](#)).

Nomogram construction and validation

We established a nomogram according to the clinical signature and rad-signature ([Figure 5](#)). In the training set, the AUC of the nomogram was 1.000 (95%CI: 1.000-1.000), while in the test set, the AUC was 0.893 (95%CI: 0.803-0.991). The AUCs of the clinical signature alone were 0.937 (95%CI: 0.868-1.000) and 0.696 (95%CI: 0.440-0.953) in the training set and test set, respectively ([Figure 6](#)). The AUC of the nomogram was greater than the AUC values of the clinical signature and rad-signature. The Hosmer-Lemeshow goodness-of-fit test was used to evaluate the calibration ability of the nomogram. The Hosmer-Lemeshow P value was $0.9 > 0.05$ in the training set and $P = 0.17 > 0.05$ in the test set, which indicates that the difference between the predicted value of the nomogram and the actual observed value was not statistically significant and that the nomogram had good calibration ability. Decision curve analysis revealed that the nomogram had a greater net benefit rate than did the rad-signature or clinical signature ([Figure 7](#)).

Table 2 Baseline characteristics of enrolled advanced gastric cancer patients in the training cohort and test cohorts, *n* (%)

| Characteristics | Total (<i>n</i> = 60) | Training (<i>n</i> = 42) | Test (<i>n</i> = 18) | <i>P</i> value |
|----------------------------------|------------------------|---------------------------|-----------------------|----------------|
| Age (years), average (mean ± SD) | 58.37 (11.846) | 58.26 (11.847) | 58.6 (12.186) | 0.918 |
| Sex | | | | 0.945 |
| Male | 47 (78.3) | 33 (78.6) | 14 (77.8) | |
| Female | 13 (21.7) | 9 (21.4) | 4 (22.2) | |
| Treatment cycles | | | | 0.201 |
| 2 | 10 (16.7) | 5 (11.9) | 5 (27.8) | |
| 3 | 29 (48.3) | 23 (54.8) | 6 (33.3) | |
| 4 + | 21 (35) | 14 (33.3) | 7 (38.9) | |
| Differentiation | | | | 0.642 |
| High | 2 (3.3) | 2 (4.8) | 0 (0.0) | |
| Moderate | 16 (26.7) | 11 (26.2) | 5 (27.8) | |
| Poor | 42 (70) | 29 (69.0) | 13 (72.2) | |
| Primary tumor location | | | | 0.467 |
| Cardia | 11 (18.3) | 9 (21.4) | 2 (11.1) | |
| Body | 22 (36.7) | 13 (31.0) | 9 (50.0) | |
| Antrum | 18 (30.0) | 14 (33.3) | 4 (22.2) | |
| Horn | 9 (15.0) | 6 (14.3) | 3 (16.7) | |
| PD-L1(22C3) CPS | | | | 0.767 |
| ≥ 5 | 36 (60.0) | 24 (57.1) | 12 (66.7) | |
| < 5 | 24 (40.0) | 18 (42.9) | 6 (33.3) | |
| CEA, median (IQR) | 3.54 (1.41-11.09) | 3.51 (1.49-11.74) | 4.75 (2.10-7.89) | 0.959 |
| CA199, median (IQR) | 14.63 (7.36-33.39) | 16.37 (7.59-36.25) | 11.13 (4.92-26.16) | 0.948 |
| T stage | | | | 0.456 |
| 1 | 4 (6.7) | 4 (9.5) | 0 (0) | |
| 2 | 5 (8.3) | 4 (9.5) | 1 (5.6) | |
| 3 | 21 (35.0) | 13 (30.9) | 8 (44.4) | |
| 4 | 30 (50.0) | 21 (50.0) | 9 (50.0) | |
| N stage | | | | 0.344 |
| 0 | 1 (1.7) | 0 (0) | 1 (5.6) | |
| 1 | 29 (48.3) | 22 (52.4) | 7 (38.9) | |
| 2 | 22 (36.7) | 14 (33.3) | 8 (44.4) | |
| 3 | 8 (13.3) | 6 (14.3) | 2 (11.1) | |

The *P* value indicates a statistically significant difference between the responder and non-responder groups ($P < 0.05$). Responders: Patients with tumor regression grade 0-1 grade; Non-responders: Patients with tumor regression grade 2-3 grade; IQR: Interquartile range; CEA: Carcinoembryonic antigen; CA199: Carbohydrate antigen 19-9; PD-L1: Programmed death-ligand 1; CPS: Combined positive score.

DISCUSSION

In this study, we developed and validated a prediction nomogram based on a rad-signature and a clinical signature to assess the TRG in AGC patients receiving nICT. The nomogram showed strong performance in predicting the TRG in both the training (AUC = 1.000) and internal test (AUC = 0.893) cohorts. This study represents the first application of radiomics for predicting the nICT response in AGC patients.

Theoretically, the neoadjuvant tumor microenvironment is the ideal situation for immunotherapy because of an intact immune system, adequate neoantigen, and low tumor cloning rates. Studies based on neoadjuvant chemotherapy in

Table 3 Comparison of radiomic models based on various machine learning methods

| Radiomic model | | Accuracy | AUC | 95%CI | Sensitivity | Specificity | PPV | NPV |
|----------------|-------|----------|-------|---------------|-------------|-------------|-------|-------|
| LR | Train | 0.976 | 1 | 1.0000-1.0000 | 0.909 | 1 | 1 | 0.969 |
| | Test | 0.778 | 0.786 | 0.4783-1.0000 | 0.5 | 0.857 | 0.5 | 0.857 |
| SVM | Train | 0.976 | 1 | 1.0000-1.0000 | 0.909 | 1 | 1 | 0.969 |
| | Test | 0.722 | 0.75 | 0.4478-1.0000 | 0.5 | 0.786 | 0.4 | 0.846 |
| KNN | Train | 0.81 | 0.897 | 0.8034-0.9913 | 0.545 | 0.903 | 0.667 | 0.848 |
| | Test | 0.778 | 0.821 | 0.6369-1.0000 | 0.5 | 0.857 | 0.5 | 0.857 |
| RF | Train | 0.976 | 1 | 1.0000-1.0000 | 0.909 | 1 | 1 | 0.969 |
| | Test | 0.833 | 0.679 | 0.2120-1.0000 | 0.25 | 1 | 1 | 0.824 |
| Extra trees | Train | 0.976 | 1 | 1.0000-1.0000 | 0.909 | 1 | 1 | 0.969 |
| | Test | 0.722 | 0.616 | 0.2080-1.0000 | 0.25 | 0.857 | 0.333 | 0.8 |
| XGBoost | Train | 0.976 | 1 | 1.0000-1.0000 | 0.909 | 1 | 1 | 0.969 |
| | Test | 0.833 | 0.75 | 0.4352-1.0000 | 0.25 | 1 | 1 | 0.824 |
| MLP | Train | 0.952 | 0.997 | 0.9889-1.0000 | 0.909 | 0.968 | 0.909 | 0.968 |
| | Test | 0.722 | 0.768 | 0.4914-1.0000 | 0.5 | 0.786 | 0.4 | 0.846 |

NPV: Negative predictive value; PPV: Positive predictive value; CI: Confidence interval; AUC: Area under the curve; LR: Logistic regression; KNN: K-nearest neighbor classification; RF: Random forest; XGBoost: EXtreme gradient boosting; MLP: Multilayer perceptron; SVM: Support vector machine.

Table 4 Comparison of clinical models based on various machine learning methods

| Clinical model | | Accuracy | AUC | 95%CI | Sensitivity | Specificity | PPV | NPV |
|----------------|-------|----------|-------|---------------|-------------|-------------|-------|-------|
| LR | Train | 0.81 | 0.837 | 0.6807-0.9938 | 0.636 | 0.871 | 0.636 | 0.871 |
| | Test | 0.278 | 0.482 | 0.1362-0.8281 | 0.75 | 0.143 | 0.2 | 0.667 |
| SVM | Train | 0.238 | 0.151 | 0.0000-0.3234 | 0.909 | 0 | 0.244 | 0 |
| | Test | 0.444 | 0.571 | 0.2439-0.8990 | 0.75 | 0.357 | 0.25 | 0.833 |
| KNN | Train | 0.786 | 0.787 | 0.6543-0.9205 | 0.182 | 1 | 1 | 0.775 |
| | Test | 0.722 | 0.607 | 0.3612-0.8531 | 0.25 | 0.857 | 0.333 | 0.8 |
| RF | Train | 0.929 | 0.993 | 0.9763-1.0000 | 0.818 | 0.968 | 0.9 | 0.937 |
| | Test | 0.556 | 0.688 | 0.4253-0.9497 | 0.75 | 0.5 | 0.3 | 0.875 |
| Extra trees | Train | 0.976 | 0.999 | 0.9945-1.0000 | 0.909 | 1 | 1 | 0.969 |
| | Test | 0.611 | 0.589 | 0.2299-0.9487 | 0.5 | 0.643 | 0.286 | 0.818 |
| XGBoost | Train | 0.857 | 0.937 | 0.8683-1.0000 | 0.818 | 0.871 | 0.692 | 0.931 |
| | Test | 0.667 | 0.696 | 0.4403-0.9526 | 0.5 | 0.714 | 0.333 | 0.833 |
| MLP | Train | 0.833 | 0.82 | 0.6535-0.9858 | 0.727 | 0.871 | 0.667 | 0.9 |
| | Test | 0.722 | 0.429 | 0.0520-0.8052 | 0 | 0.929 | 0 | 0.765 |

NPV: Negative predictive value; PPV: Positive predictive value; CI: Confidence interval; AUC: Area under the curve; LR: Logistic regression; KNN: K-nearest neighbor classification; RF: Random forest; XGBoost: EXtreme gradient boosting; MLP: Multilayer perceptron; SVM: Support vector machine.

combination with ICI therapy have been successful in treating resectable non-small cell lung cancer[29]. In the CheckMate 649 trial, compared with chemotherapy alone, nivolumab combined with chemotherapy significantly improved OS and PFS in patients with metastatic gastric and gastroesophageal junction cancers. This combination was recommended as a first-line treatment for patients in the PD-L1 ≥ 5 subgroup[6]. The NEONIPIGA study revealed that neoadjuvant therapy with ravulizumab and ipilimumab is feasible and results in a high pCR rate in patients with resectable adenocarcinoma of the gastroesophageal junction who have mismatch repair-deficient or microsatellite instability-high tumors[30]. A recent phase II single-arm clinical trial revealed that neoadjuvant chemotherapy with tislelizumab in combination with the S-1

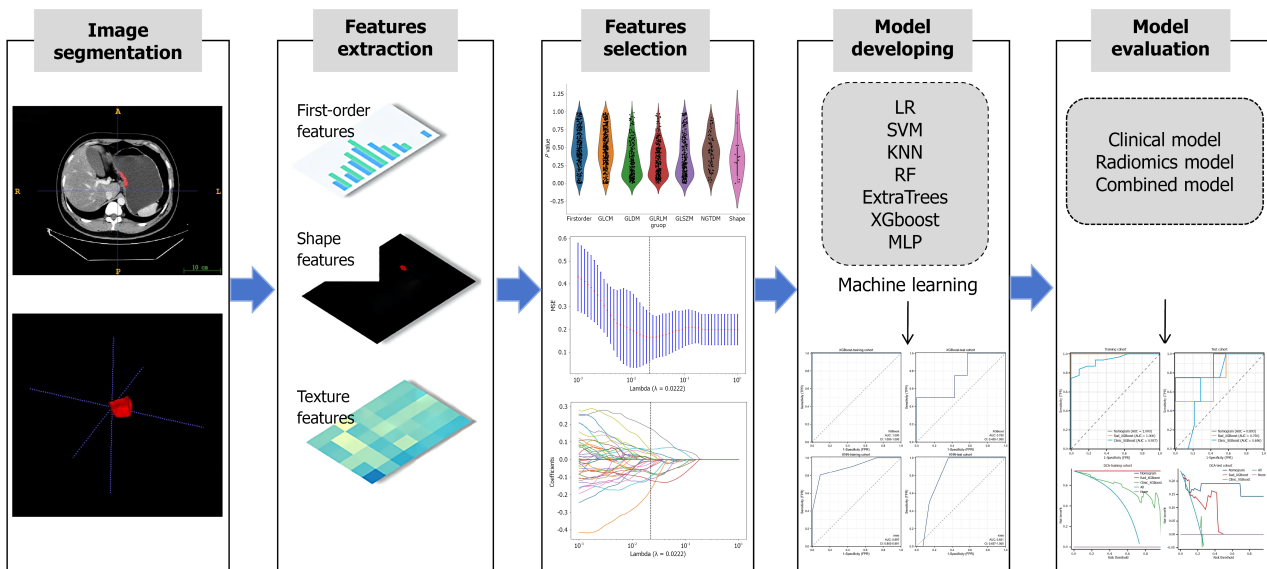


Figure 2 A flow chart of the radiomic analysis. According to the computed tomography images, important imaging features were screened and combined with important clinical risk factors to generate a radiomic nomogram. The performance and clinical utility of the radiomic model in predicting the response of patients with advanced gastric cancer to neoadjuvant immunochemotherapy were evaluated through receiver operating characteristic curve analysis and decision curve analysis. LR: Logistic regression; KNN: K-nearest neighbor classification; RF: Random forest; XGBoost: Extreme gradient boosting; MLP: Multilayer perceptron; SVM: Support vector machine; MSE: Mean squared error; TPR: True positive rate; FPR: False positive rate; DCA: Decision curve analysis.

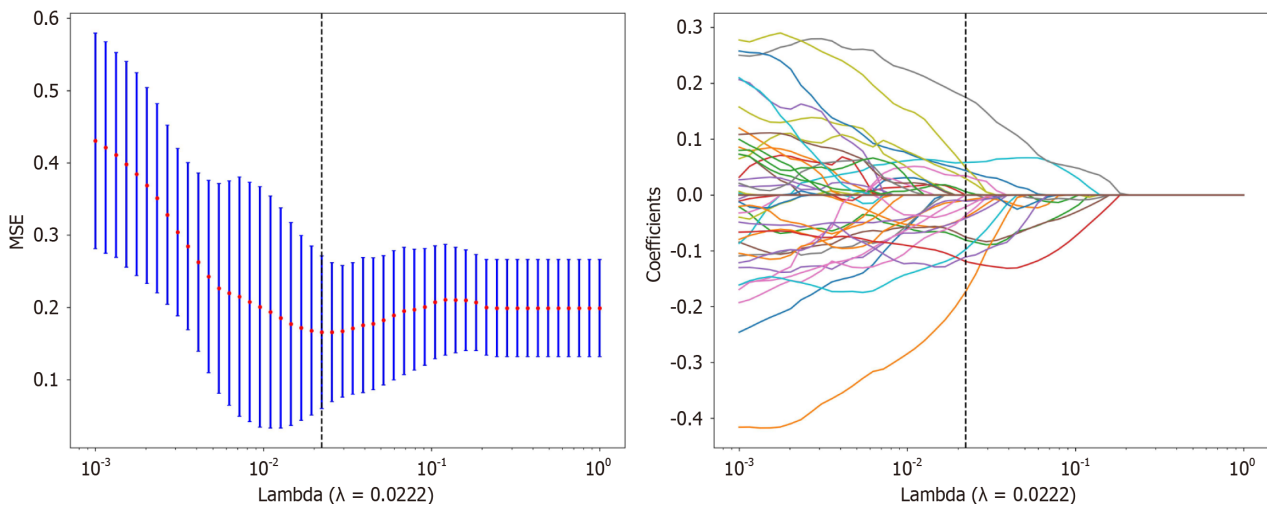


Figure 3 Least absolute shrinkage and selection operator regression was used to screen for radiomic features. MSE: Mean squared error.

combined with oxaliplatin regimen has promising application in gastric and gastroesophageal junction cancers, with pCR and MPR rates reaching 25% and 53.1%, respectively[31]. Moreover, a recent study showed that for locally AGC, nICT can lead to higher gastric resection rates and better tumor regression than chemotherapy alone[32].

Clinically, nICT has been universally applied in the treatment of AGC. Nevertheless, the efficiency of nICT is widely divergent, and the long-term survival of patients who benefit from nICT is extraordinarily superior to that of patients who do not benefit[33]. The lack of reliable and effective methods for predicting sensitivity to nICT hinders the development of therapeutic strategies. If a patient is insensitive to nICT, ineffective and unnecessary treatments may be continued, whereas if the patient misses the opportunity for radical resection due to disease progression during nICT, admission to the hospital and cost are wasted. Therefore, the establishment of an effective prediction model that can predict sensitivity to nICT before nICT is administered is highly important for AGC patients. RECIST 1.1 is the current standard used to evaluate the curative effect of nICT in patients with GC. However, although RECIST 1.1 is the standard, it is based on the calculation of the percentage of tumor regression, which is limited to retrospective assessments[34]. An early response in the evaluation of the treatment effect of nICT is preferable in the determination of nICT-related treatments. This not only helps to predict the prognosis of patients with early nICT but also reduces nICT-induced toxicity. Consequently, patients can benefit from a reduced presentation to the hospital and treatment costs.

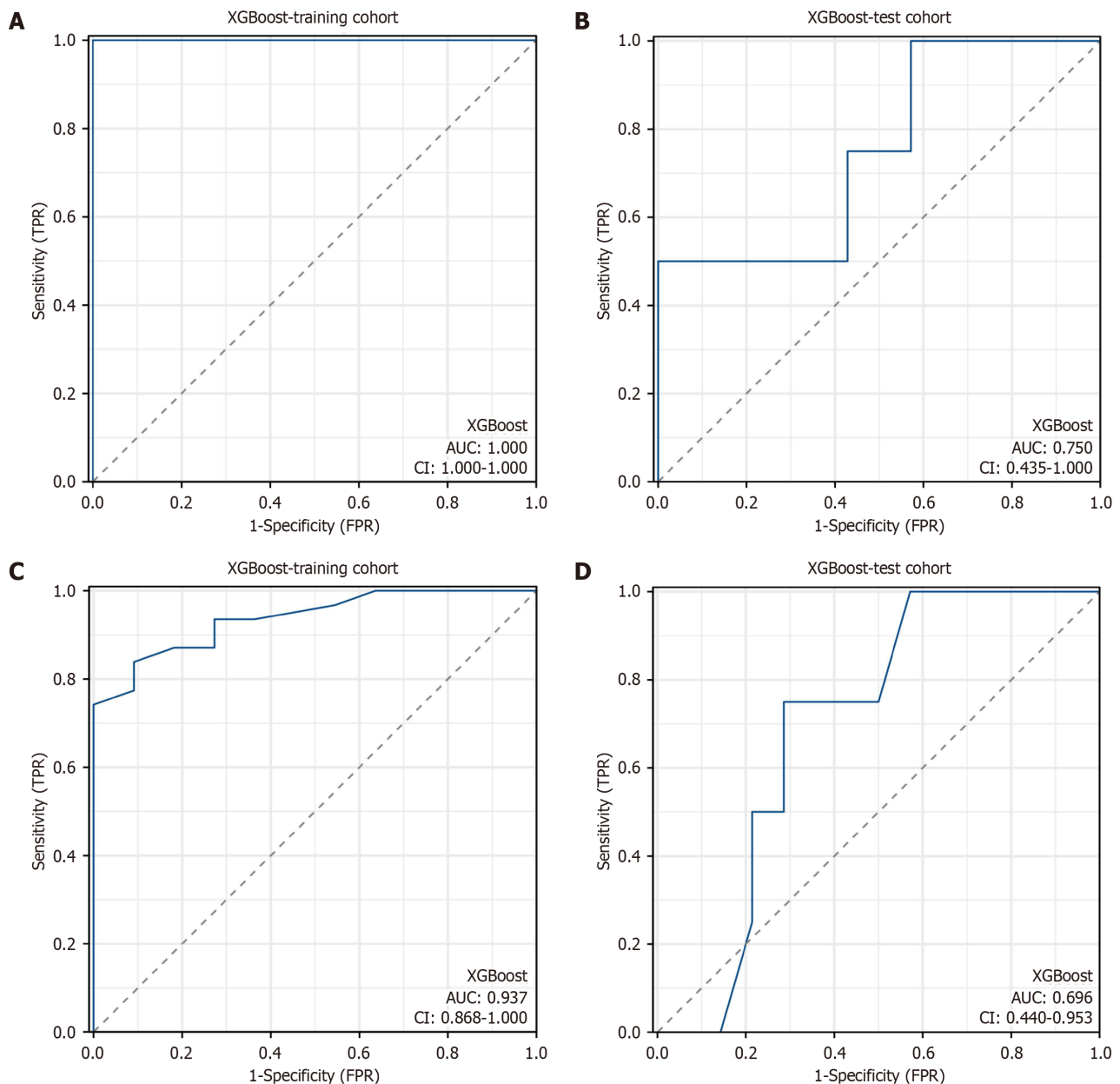


Figure 4 Receiver operating characteristic curve analysis of the radiomic model and the clinical model. A: The area under the curve (AUC) of the radiomic model was 1.000 [95% confidence interval (CI): 1.000-1.000] in the training cohort; B: The AUC of the radiomic model was 0.750 (95%CI: 0.435-1.000) in the test cohort; C: The AUC of the clinical model was 0.937 (95%CI: 0.868-1.000) in the training cohort; D: The AUC of the clinical model was 0.696 (95%CI: 0.440-0.953) in the test cohort. XGBoost: EXtreme gradient boosting; TPR: True positive rate; FPR: False positive rate.

Radiomics involves the conversion of medical images into extractable data through high-throughput extraction of quantitative features based on shape, size, volume, and other relevant factors. This approach has been demonstrated to be valuable in the examination of various pathological conditions[35,36]. Radiomic features distinguish themselves from the conventional semantic features identified by radiologists because of their capacity to provide more detailed information on tumors in a more objective manner[36].

We developed a rad-signature based on 19 radiomic features, which included 14 texture features and 5 histogram features. Among the texture features were complexity, busyness, gray level emphasis, short run emphasis, small area emphasis, gray level nonuniformity normalized, difference variance, and joint energy, all of which describe the spatial relationships of adjacent pixels[37]. These features are crucial in considering the pixels and shapes within the ROI. Additionally, the histogram features included kurtosis, mean, 90th percentile, mean absolute deviation, and minimum, which highlight the distribution pattern of gray-level pixel values within the ROI[37]. The rad-signature demonstrated accurate prediction of the nICT response, as indicated by the AUC values in both the training and test sets. Combining the rad-signature with the clinical signature resulted in improved efficacy. By integrating these radiomic features, we were able to better understand and predict the response to treatment.

For clinical factors, our study suggested that cN stage and cT stage may be independent predictors of nICT response, as corroborated by previous studies[38]. However, previous studies have also indicated that PD-L1 expression, differentiation and tumor location are important predictors of immunotherapy efficacy in patients with GC[25-27], which was not

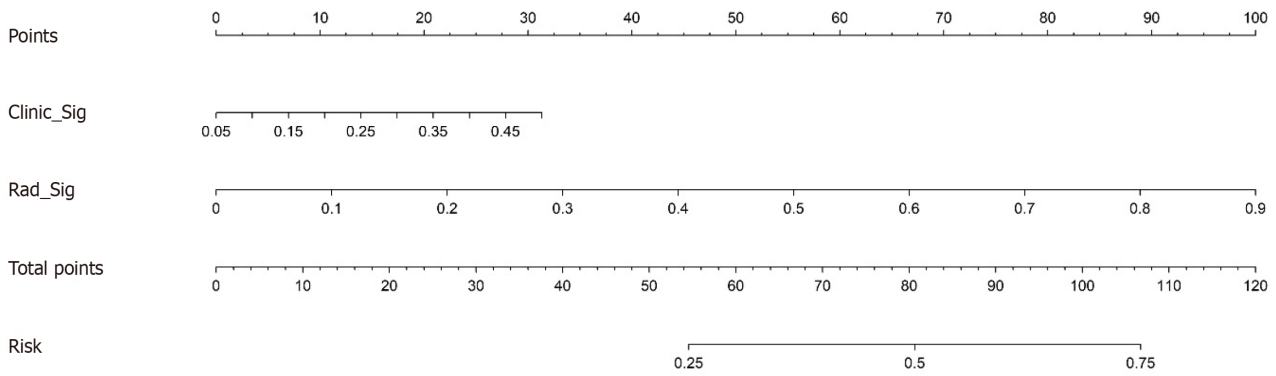


Figure 5 Radiomic nomogram for predicting the response of patients with advanced gastric cancer to neoadjuvant immunotherapy based on the radiomic signature and clinical signature. Different values for each variable correspond to a point at the top of the graph, and the sum of points for all variables corresponds to the total point. The line from the total point to the bottom is the probability of response. Response, TRG 0-1; Clinic_Sig, clinical signature; Rad_Sig, radiomic signature.

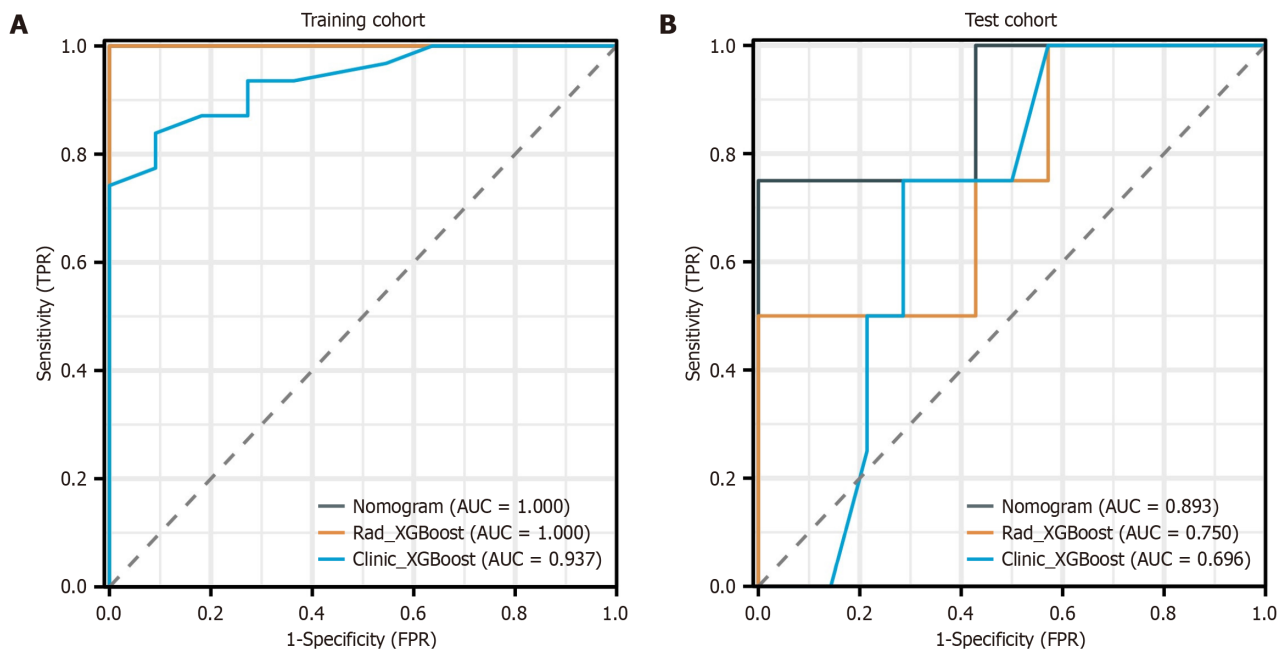


Figure 6 Operating characteristic curve analysis of the nomogram. A: Area under the curve (AUC) of 1.000 [95% confidence interval (CI): 1.000-1.000] in the training cohort of the nomogram; B: AUC of 0.893 (95%CI: 0.803-0.991) in the test cohort of the nomogram. The operating characteristic curves revealed that the AUCs of the nomogram were superior to those of both the radiomic signature and the clinical signature. AUC: Area under the curve; XGBoost: EXtreme gradient boosting; TPR: True positive rate; FPR: False positive rate.

demonstrated in our study. We believe that our sample size limitation may have contributed to this difference. Since the number of predictors selected after the univariate analysis was small and these features alone may not adequately capture the clinical status of patients or have significant clinical applicability, we included all five clinical factors in the clinical signature. The AUC values of our clinical signature were 0.937 and 0.696 in the training and testing cohorts, respectively, which indicates good efficacy. The optimal predictive performance was achieved when both clinical and CT radiomic features were included in the machine learning model, which can provide guidance for the subsequent treatment of patients.

Radiological features, which are driven by the underlying pathophysiology, can be effectively analyzed quantitatively to reveal subtle relationships between the two. Numerous studies have been conducted in recent years in which radiomics has been applied to investigate the mechanisms of the tumor response to therapy. For example, Sun *et al*[39] developed a radiomic signature associated with CD8 + T cells, which demonstrated a significant correlation with the clinical response and outcomes of patients receiving anti-PD1 immunotherapy. Jiang *et al*[40] evaluated the GC tumor microenvironment and predicted treatment response by combining radiomic features with immunohistochemistry features, and they reported that tumors with high immune cell infiltration exhibited a good response to immunotherapy. Unfortunately, we did not explore this aspect further in this study.

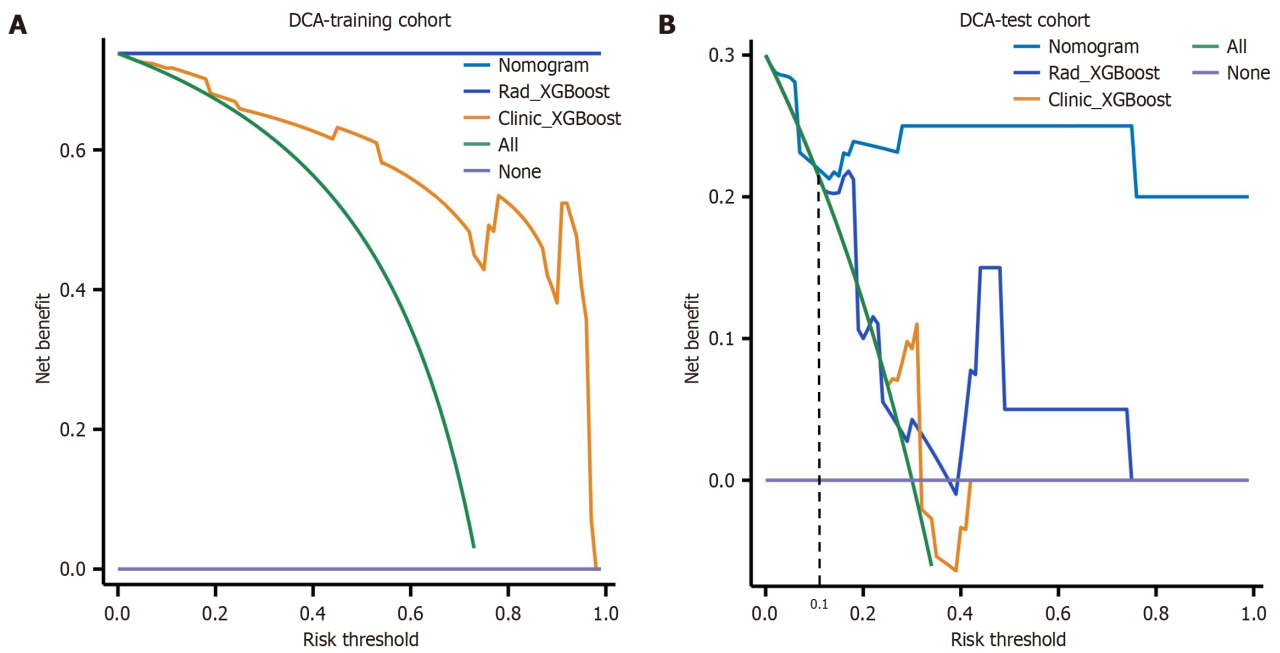


Figure 7 Decision curves were generated to compare the differences in the net benefit of the various models. A: Decision curves in the training cohort; B: Decision curves in the test cohort. The X-axis indicates the threshold probability, and the Y-axis indicates the net benefit. The decision curve revealed that when the threshold probability exceeded 10%, the net benefit of the clinical application of the nomogram exceeded that of the other models in the test cohort. XGBoost: EXtreme gradient boosting; DCA: Decision curve analysis.

This study has several limitations: (1) It is a single-center retrospective study with a limited sample size ($n = 60$), therefore, the generalizability of the results is limited, and further validation is needed in a multicenter prospective cohort study; (2) Potential bias may be introduced by the use of different nICT regimens, thus, the sample size should be increased and stratified for analysis; and (3) The delineation of the ROI is subjective, which may have led to potential bias in the results, the establishment of an automatic or semiautomatic image analysis method is recommended to improve accuracy in future studies.

CONCLUSION

In this study, we developed and validated a CT-based nomogram for predicting the treatment response of patients with AGC to nICT. Our findings suggest that this nomogram holds promise as a tool for evaluating prognosis and informing clinical decision-making regarding AGC patients.

FOOTNOTES

Author contributions: Wang HJ and Zhang BY significantly contributed to the study design; Zhang J and Wang Q contributed to the data collection, data interpretation, and data analyses and drafted the manuscript; Yu YM, Guo TH, Wang RF and Gao W managed the clinical information and statistical analyses; Yu HL and Chen JJ contributed to image segmentation; Sun LL contributed to the confirmation of tumor regression grading; All the authors have read and approved the final manuscript.

Supported by the Affiliated Hospital of Qingdao University Horizontal Fund, No. 3635; and Intramural Project Fund, No. 4618.

Institutional review board statement: The study was reviewed and approved by the Affiliated Hospital of Qingdao University] Institutional Review Board, Approval No. QYFYWZLL28662.

Informed consent statement: Informed consent requirement was waived due to the retrospective nature of the study.

Conflict-of-interest statement: The authors declare that they have no conflict of interest.

Data sharing statement: Please contact the corresponding author for data requests.

Open-Access: This article is an open-access article that was selected by an in-house editor and fully peer-reviewed by external reviewers. It is distributed in accordance with the Creative Commons Attribution NonCommercial (CC BY-NC 4.0) license, which permits others to distribute, remix, adapt, build upon this work non-commercially, and license their derivative works on different terms, provided the original work is properly cited and the use is non-commercial. See: <https://creativecommons.org/licenses/by-nc/4.0/>

Country of origin: China

ORCID number: Jun Zhang 0009-0001-4978-8877; Hai-Ji Wang 0009-0003-3489-0822.

S-Editor: Fan M

L-Editor: A

P-Editor: Zhang L

REFERENCES

- 1 **Bray F**, Laversanne M, Sung H, Ferlay J, Siegel RL, Soerjomataram I, Jemal A. Global cancer statistics 2022: GLOBOCAN estimates of incidence and mortality worldwide for 36 cancers in 185 countries. *CA Cancer J Clin* 2024; **74**: 229-263 [PMID: 38572751 DOI: 10.3322/caac.21834]
- 2 **Smyth EC**, Nilsson M, Grabsch HI, van Grieken NC, Lordick F. Gastric cancer. *Lancet* 2020; **396**: 635-648 [PMID: 32861308 DOI: 10.1016/S0140-6736(20)31288-5]
- 3 **Japanese Gastric Cancer Association**. Japanese gastric cancer treatment guidelines 2018 (5th edition). *Gastric Cancer* 2021; **24**: 1-21 [PMID: 32060757 DOI: 10.1007/s10120-020-01042-y]
- 4 **Wang FH**, Zhang XT, Li YF, Tang L, Qu XJ, Ying JE, Zhang J, Sun LY, Lin RB, Qiu H, Wang C, Qiu MZ, Cai MY, Wu Q, Liu H, Guan WL, Zhou AP, Zhang YJ, Liu TS, Bi F, Yuan XL, Rao SX, Xin Y, Sheng WQ, Xu HM, Li GX, Ji JF, Zhou ZW, Liang H, Zhang YQ, Jin J, Shen L, Li J, Xu RH. The Chinese Society of Clinical Oncology (CSCO): Clinical guidelines for the diagnosis and treatment of gastric cancer, 2021. *Cancer Commun (Lond)* 2021; **41**: 747-795 [PMID: 34197702 DOI: 10.1002/cac2.12193]
- 5 **Schaft N**, Dörrie J, Schuler G, Schuler-Thurner B, Sallam H, Klein S, Eisenberg G, Frankenburg S, Lotem M, Khatib A. The future of affordable cancer immunotherapy. *Front Immunol* 2023; **14**: 1248867 [PMID: 37736099 DOI: 10.3389/fimmu.2023.1248867]
- 6 **Janjigian YY**, Shitara K, Moehler M, Garrido M, Salman P, Shen L, Wyrwicz L, Yamaguchi K, Skoczylas T, Campos Bragagnoli A, Liu T, Schenker M, Yanez P, Tehfe M, Kowalyszyn R, Karamouzis MV, Bruges R, Zander T, Pazo-Cid R, Hitre E, Feeney K, Cleary JM, Poulart V, Cullen D, Lei M, Xiao H, Kondo K, Li M, Ajani JA. First-line nivolumab plus chemotherapy versus chemotherapy alone for advanced gastric, gastro-oesophageal junction, and oesophageal adenocarcinoma (CheckMate 649): a randomised, open-label, phase 3 trial. *Lancet* 2021; **398**: 27-40 [PMID: 34102137 DOI: 10.1016/S0140-6736(21)00797-2]
- 7 **Xu J**, Jiang H, Pan Y, Gu K, Cang S, Han L, Shu Y, Li J, Zhao J, Pan H, Luo S, Qin Y, Guo Q, Bai Y, Ling Y, Yang J, Yan Z, Yang L, Tang Y, He Y, Zhang L, Liang X, Niu Z, Zhang J, Mao Y, Guo Y, Peng B, Li Z, Liu Y, Wang Y, Zhou H; ORIENT-16 Investigators. Sintilimab Plus Chemotherapy for Unresectable Gastric or Gastroesophageal Junction Cancer: The ORIENT-16 Randomized Clinical Trial. *JAMA* 2023; **330**: 2064-2074 [PMID: 38051328 DOI: 10.1001/jama.2023.19918]
- 8 **Fuchs CS**, Doi T, Jang RW, Muro K, Satoh T, Machado M, Sun W, Jalal SI, Shah MA, Metges JP, Garrido M, Golan T, Mandala M, Wainberg ZA, Catenacci DV, Ohtsu A, Shitara K, Geva R, Bleeker J, Ko AH, Ku G, Philip P, Enzinger PC, Bang YJ, Levitan D, Wang J, Rosales M, Dalal RP, Yoon HH. Safety and Efficacy of Pembrolizumab Monotherapy in Patients With Previously Treated Advanced Gastric and Gastroesophageal Junction Cancer: Phase 2 Clinical KEYNOTE-059 Trial. *JAMA Oncol* 2018; **4**: e180013 [PMID: 29543932 DOI: 10.1001/jamaoncol.2018.0013]
- 9 **Muro K**, Chung HC, Shankaran V, Geva R, Catenacci D, Gupta S, Eder JP, Golan T, Le DT, Burtness B, McRee AJ, Lin CC, Pathiraja K, Lunceford J, Emancipator K, Juco J, Koshiji M, Bang YJ. Pembrolizumab for patients with PD-L1-positive advanced gastric cancer (KEYNOTE-012): a multicentre, open-label, phase 1b trial. *Lancet Oncol* 2016; **17**: 717-726 [PMID: 27157491 DOI: 10.1016/S1470-2045(16)00175-3]
- 10 **Xu H**, Li T, Shao G, Wang W, He Z, Xu J, Qian Y, Liu H, Ge H, Wang L, Zhang D, Yang L, Li F, Xu Z. Evaluation of neoadjuvant immunotherapy plus chemotherapy in Chinese surgically resectable gastric cancer: a pilot study by meta-analysis. *Front Immunol* 2023; **14**: 1193614 [PMID: 37426646 DOI: 10.3389/fimmu.2023.1193614]
- 11 **Seymour L**, Bogaerts J, Perrone A, Ford R, Schwartz LH, Mandrekar S, Lin NU, Litière S, Dancy J, Chen A, Hodi FS, Therasse P, Hoekstra OS, Shankar LK, Wolchok JD, Ballinger M, Caramella C, de Vries EGE; RECIST working group. iRECIST: guidelines for response criteria for use in trials testing immunotherapeutics. *Lancet Oncol* 2017; **18**: e143-e152 [PMID: 28271869 DOI: 10.1016/S1470-2045(17)30074-8]
- 12 **Gillies RJ**, Kinahan PE, Hricak H. Radiomics: Images Are More than Pictures, They Are Data. *Radiology* 2016; **278**: 563-577 [PMID: 26579733 DOI: 10.1148/radiol.2015151169]
- 13 **Granzier RWY**, van Nijnatten TJA, Woodruff HC, Smidt ML, Lobbes MBI. Exploring breast cancer response prediction to neoadjuvant systemic therapy using MRI-based radiomics: A systematic review. *Eur J Radiol* 2019; **121**: 108736 [PMID: 31734639 DOI: 10.1016/j.ejrad.2019.108736]
- 14 **Chen M**, Copley SJ, Viola P, Lu H, Aboagye EO. Radiomics and artificial intelligence for precision medicine in lung cancer treatment. *Semin Cancer Biol* 2023; **93**: 97-113 [PMID: 37211292 DOI: 10.1016/j.semcancer.2023.05.004]
- 15 **Jin J**, Jiang Y, Zhao YL, Huang PT. Radiomics-based Machine Learning to Predict the Recurrence of Hepatocellular Carcinoma: A Systematic Review and Meta-analysis. *Acad Radiol* 2024; **31**: 467-479 [PMID: 37867018 DOI: 10.1016/j.acra.2023.09.008]
- 16 **Cui J**, Li L, Liu N, Hou W, Dong Y, Yang F, Zhu S, Li J, Yuan S. Model integrating CT-based radiomics and genomics for survival prediction in esophageal cancer patients receiving definitive chemoradiotherapy. *Biomark Res* 2023; **11**: 44 [PMID: 37095586 DOI: 10.1186/s40364-023-00480-x]
- 17 **Xu Q**, Sun Z, Li X, Ye C, Zhou C, Zhang L, Lu G. Advanced gastric cancer: CT radiomics prediction and early detection of downstaging with neoadjuvant chemotherapy. *Eur Radiol* 2021; **31**: 8765-8774 [PMID: 33909133 DOI: 10.1007/s00330-021-07962-2]
- 18 **Park KJ**, Lee JL, Yoon SK, Heo C, Park BW, Kim JK. Radiomics-based prediction model for outcomes of PD-1/PD-L1 immunotherapy in metastatic urothelial carcinoma. *Eur Radiol* 2020; **30**: 5392-5403 [PMID: 32394281 DOI: 10.1007/s00330-020-06847-0]
- 19 **Yoon SH**, Kim YH, Lee YJ, Park J, Kim JW, Lee HS, Kim B. Tumor Heterogeneity in Human Epidermal Growth Factor Receptor 2 (HER2)-Positive Advanced Gastric Cancer Assessed by CT Texture Analysis: Association with Survival after Trastuzumab Treatment. *PLoS One* 2016; **11**: e0161278 [PMID: 27517841 DOI: 10.1371/journal.pone.0161278]

- 20 **Li J**, Chen Z, Chen Y, Zhao J, He M, Li X, Zhang L, Dong B, Zhang X, Tang L, Shen L. CT-based delta radiomics in predicting the prognosis of stage IV gastric cancer to immune checkpoint inhibitors. *Front Oncol* 2022; **12**: 1059874 [PMID: 36686828 DOI: 10.3389/fonc.2022.1059874]
- 21 **Li J**, Zhang HL, Yin HK, Zhang HK, Wang Y, Xu SN, Ma F, Gao JB, Li HL, Qu JR. Comparison of MRI and CT-Based Radiomics and Their Combination for Early Identification of Pathological Response to Neoadjuvant Chemotherapy in Locally Advanced Gastric Cancer. *J Magn Reson Imaging* 2023; **58**: 907-923 [PMID: 36527425 DOI: 10.1002/jmri.28570]
- 22 **Sun KY**, Hu HT, Chen SL, Ye JN, Li GH, Chen LD, Peng JJ, Feng ST, Yuan YJ, Hou X, Wu H, Li X, Wu TF, Wang W, Xu JB. CT-based radiomics scores predict response to neoadjuvant chemotherapy and survival in patients with gastric cancer. *BMC Cancer* 2020; **20**: 468 [PMID: 32450841 DOI: 10.1186/s12885-020-06970-7]
- 23 **Zeng Q**, Zhu Y, Li L, Feng Z, Shu X, Wu A, Luo L, Cao Y, Tu Y, Xiong J, Zhou F, Li Z. CT-based radiomic nomogram for preoperative prediction of DNA mismatch repair deficiency in gastric cancer. *Front Oncol* 2022; **12**: 883109 [PMID: 36185292 DOI: 10.3389/fonc.2022.883109]
- 24 **Li M**, Li X, Guo Y, Miao Z, Liu X, Guo S, Zhang H. Development and assessment of an individualized nomogram to predict colorectal cancer liver metastases. *Quant Imaging Med Surg* 2020; **10**: 397-414 [PMID: 32190566 DOI: 10.21037/qims.2019.12.16]
- 25 **Kong J**, Ha D, Lee J, Kim I, Park M, Im SH, Shin K, Kim S. Network-based machine learning approach to predict immunotherapy response in cancer patients. *Nat Commun* 2022; **13**: 3703 [PMID: 35764641 DOI: 10.1038/s41467-022-31535-6]
- 26 **Zhou CQ**, Gao D, Gui Y, Li NP, Guo WW, Zhou HY, Li R, Chen J, Zhang XM, Chen TW. Computed tomography-based nomogram of Siewert type II/III adenocarcinoma of esophagogastric junction to predict response to docetaxel, oxaliplatin and S-1. *World J Radiol* 2024; **16**: 9-19 [PMID: 38312347 DOI: 10.4329/wjr.v16.i1.9]
- 27 **Chen D**, Fu M, Chi L, Lin L, Cheng J, Xue W, Long C, Jiang W, Dong X, Sui J, Lin D, Lu J, Zhuo S, Liu S, Li G, Chen G, Yan J. Prognostic and predictive value of a pathomics signature in gastric cancer. *Nat Commun* 2022; **13**: 6903 [PMID: 36371443 DOI: 10.1038/s41467-022-34703-w]
- 28 **Kocak B**, Baessler B, Bakas S, Cuocolo R, Fedorov A, Maier-Hein L, Mercaldo N, Müller H, Orlhac F, Pinto Dos Santos D, Stanzione A, Uggla L, Zwanenburg A. CheckList for EvaluAtion of Radiomics research (CLEAR): a step-by-step reporting guideline for authors and reviewers endorsed by ESR and EuSoMI. *Insights Imaging* 2023; **14**: 75 [PMID: 37142815 DOI: 10.1186/s13244-023-01415-8]
- 29 **Forde PM**, Chaft JE, Smith KN, Anagnostou V, Cottrell TR, Hellmann MD, Zahurak M, Yang SC, Jones DR, Broderick S, Battafarano RJ, Velez MJ, Rektman N, Olah Z, Naidoo J, Marrone KA, Verde F, Guo H, Zhang J, Caushi JX, Chan HY, Sidhom JW, Scharpf RB, White J, Gabrielson E, Wang H, Rosner GL, Rusch V, Wolchok JD, Merghoub T, Taube JM, Velculescu VE, Topalian SL, Brahmer JR, Pardoll DM. Neoadjuvant PD-1 Blockade in Resectable Lung Cancer. *N Engl J Med* 2018; **378**: 1976-1986 [PMID: 29658848 DOI: 10.1056/NEJMoa1716078]
- 30 **André T**, Tougeron D, Piessen G, de la Fouchardière C, Louvet C, Adenis A, Jary M, Tournigand C, Aparicio T, Desrame J, Lièvre A, Garcia-Larnicol ML, Pudlzar T, Cohen R, Memmi S, Vernerey D, Henriques J, Lefevre JH, Svrcek M. Neoadjuvant Nivolumab Plus Ipilimumab and Adjuvant Nivolumab in Localized Deficient Mismatch Repair/Microsatellite Instability-High Gastric or Esophagogastric Junction Adenocarcinoma: The GERCOR NEONIPIGA Phase II Study. *J Clin Oncol* 2023; **41**: 255-265 [PMID: 35969830 DOI: 10.1200/JCO.22.00686]
- 31 **Yin Y**, Lin Y, Yang M, Lv J, Liu J, Wu K, Liu K, Li A, Shuai X, Cai K, Wang Z, Wang G, Shen J, Zhang P, Tao K. Neoadjuvant tislelizumab and tegafur/gimeracil/oteracil (S-1) plus oxaliplatin in patients with locally advanced gastric or gastroesophageal junction cancer: Early results of a phase 2, single-arm trial. *Front Oncol* 2022; **12**: 959295 [PMID: 36158692 DOI: 10.3389/fonc.2022.959295]
- 32 **Lin JL**, Lin JX, Lin JP, Zheng CH, Li P, Xie JW, Wang JB, Lu J, Chen QY, Huang CM. Safety and Efficacy of Camrelizumab in Combination With Nab-Paclitaxel Plus S-1 for the Treatment of Gastric Cancer With Serosal Invasion. *Front Immunol* 2021; **12**: 783243 [PMID: 35116023 DOI: 10.3389/fimmu.2021.783243]
- 33 **Tan X**, Yang X, Hu S, Ge Y, Wu Q, Wang J, Sun Z. Prediction of response to neoadjuvant chemotherapy in advanced gastric cancer: A radiomics nomogram analysis based on CT images and clinicopathological features. *J Xray Sci Technol* 2023; **31**: 49-61 [PMID: 36314190 DOI: 10.3233/XST-221291]
- 34 **Eisenhauer EA**, Therasse P, Bogaerts J, Schwartz LH, Sargent D, Ford R, Dancey J, Arbuck S, Gwyther S, Mooney M, Rubinstein L, Shankar L, Dodd L, Kaplan R, Lacombe D, Verweij J. New response evaluation criteria in solid tumours: revised RECIST guideline (version 1.1). *Eur J Cancer* 2009; **45**: 228-247 [PMID: 19097774 DOI: 10.1016/j.ejca.2008.10.026]
- 35 **Salvatore C**, Castiglioni I, Cerasa A. Radiomics approach in the neurodegenerative brain. *Aging Clin Exp Res* 2021; **33**: 1709-1711 [PMID: 31428998 DOI: 10.1007/s40520-019-01299-z]
- 36 **Mayerhoefer ME**, Materka A, Langs G, Häggström I, Szczypiński P, Gibbs P, Cook G. Introduction to Radiomics. *J Nucl Med* 2020; **61**: 488-495 [PMID: 32060219 DOI: 10.2967/jnumed.118.222893]
- 37 **Zwanenburg A**, Vallières M, Abdalah MA, Aerts HJWL, Andrearczyk V, Apte A, Ashrafinia S, Bakas S, Beukinga RJ, Boellaard R, Bogowicz M, Boldrini L, Buvat I, Cook GJR, Davatzikos C, Depeursinge A, Desserot MC, Dinapoli N, Dinh CV, Echegaray S, El Naqa I, Fedorov AY, Gatta R, Gillies RJ, Goh V, Götz M, Guckenberger M, Ha SM, Hatt M, Isensee F, Lambin P, Leger S, Leijenaar RTH, Lenkowitz J, Lippert F, Lodsnegård A, Maier-Hein KH, Morin O, Müller H, Napel S, Nioche C, Orlhac F, Pati S, Pfaehler EAG, Rahmim A, Rao AUK, Scherer J, Siddique MM, Sijtsema NM, Socarras Fernandez J, Spezi E, Steenbakkers RJHM, Tanadini-Lang S, Thorwarth D, Troost EGC, Upadhadaya T, Valentini V, van Dijk LV, van Griethuysen J, van Velden FHP, Whybra P, Richter C, Löck S. The Image Biomarker Standardization Initiative: Standardized Quantitative Radiomics for High-Throughput Image-based Phenotyping. *Radiology* 2020; **295**: 328-338 [PMID: 32154773 DOI: 10.1148/radiol.2020191145]
- 38 **Shin K**, Park SJ, Lee J, Park CH, Song KY, Lee HH, Seo HS, Jung YJ, Park JM, Lee SH, Roh SY, Kim IH. Efficacy of capecitabine and oxaliplatin versus S-1 as adjuvant chemotherapy in gastric cancer after D2 lymph node dissection according to lymph node ratio and N stage. *BMC Cancer* 2019; **19**: 1232 [PMID: 31852475 DOI: 10.1186/s12885-019-6433-3]
- 39 **Sun R**, Limkin EJ, Vakalopoulou M, Dercle L, Champiat S, Han SR, Verlingue L, Brandao D, Lancia A, Ammari S, Hollebécque A, Scoazec JY, Marabelle A, Massard C, Soria JC, Robert C, Paragios N, Deutsch E, Féré C. A radiomics approach to assess tumour-infiltrating CD8 cells and response to anti-PD-1 or anti-PD-L1 immunotherapy: an imaging biomarker, retrospective multicohort study. *Lancet Oncol* 2018; **19**: 1180-1191 [PMID: 30120041 DOI: 10.1016/S1470-2045(18)30413-3]
- 40 **Jiang Y**, Zhou K, Sun Z, Wang H, Xie J, Zhang T, Sang S, Islam MT, Wang JY, Chen C, Yuan Q, Xi S, Li T, Xu Y, Xiong W, Wang W, Li G, Li R. Non-invasive tumor microenvironment evaluation and treatment response prediction in gastric cancer using deep learning radiomics. *Cell Rep Med* 2023; **4**: 101146 [PMID: 37557177 DOI: 10.1016/j.xcrm.2023.101146]



Published by **Baishideng Publishing Group Inc**
7041 Koll Center Parkway, Suite 160, Pleasanton, CA 94566, USA
Telephone: +1-925-3991568
E-mail: office@baishideng.com
Help Desk: <https://www.f6publishing.com/helpdesk>
<https://www.wjgnet.com>

